Desalination and Water Treatment
www.deswater.com

doi: 10.1080/19443994.2015.1033762

57 (2016) 10295–10311
May

Taylor & Francis
Taylor & Francis Group

Removal of reactive dyes using a high throughput-hybrid separation process

Sankha Karmakar[a], Mrinmoy Mondal[a], Sourja Ghosh[b], Sibdas Bandyopadhyay[b], Swachchha Majumdar[b], Sirshendu De[a,*]

[a]*Department of Chemical Engineering, Indian Institute of Technology Kharagpur, Kharagpur 721302, India, Tel. +91 8902499547; email: sankha.karmakar@che.iitkgp.ernet.in (S. Karmakar), Tel. +91 9477076005; email: mrinmoy.mondal@che.iitkgp.ernet.in (M. Mondal), Tel. +91 3222 283926; Fax: +91 3222 255303; email: sde@che.iitkgp.ernet.in (S. De)*
[b]*Central Glass and Ceramic Research Institute, Kolkata 700032, India, Tel. +91 9432674199; email: sourja@cgcri.res.in (S. Ghosh), Tel. +91 9432800700; email: Sibdas4@rediffmail.com (S. Bandyopadhyay), Tel. +91 33 24733496, ext. 3266; email: swachchha@cgcri.res.in (S. Majumdar)*

Received 8 September 2014; Accepted 20 March 2015

ABSTRACT

Toxic and carcinogenic reactive dyes are abundantly used in textile industries due to their wide variety of colour and texture. In this study, a hybrid separation process was used to remove four common reactive dyes (reactive yellow, red, black and brown) from aqueous solution. Synthetic solution of these dyes was subjected to adsorption by activated carbon followed by microfiltration (MF), using a ceramic membrane module. Dyes were completely removed by adsorption at pH 4.5 and the dye-loaded adsorbents were removed by cross-flow MF. Maximum Langmuir adsorption capacity of activated carbon for these four dyes was in the range of 88–106 mg/g. Effects of trans-membrane pressure drop and cross-flow rate on the throughput of the combined process was investigated. Membrane fouling was due to the cake type of layer formed by the activated carbon particles. Five different washing protocols were tested for their efficiency and the acid–alkali wash was found to be the most effective.

Keywords: Ceramic membrane; Microfiltration; Adsorption; Activated carbon; Washing

1. Introduction

Textile industries produce effluent containing toxic and carcinogenic dyes. Since dyeing units require about 40–50 L of water for processing of 1 kg of cloth [1], the amount of wastewater produced is huge. A typical textile effluent contains pollutants such as sizing agents, dyes, volatile organic compounds, ethylene glycol and huge amount of salt which are resistant to various treatment processes [2–7].

Reactive dyes are mainly used to colour cotton, rayon and other cellulosic fabrics. Due to their wide variety of colour and texture, they are used abundantly. They have very poor fixation characteristics, thereby leaving substantial amount of dye in the wastewater [8], that are mostly non-degradable, toxic and carcinogenic.

Conventional methods of treatment of textile wastewater consist of chemical coagulation (using ferrous, lime and polyelectrolyte), biological treatment followed by adsorption using activated carbon [9,10]. Coagulation generates large volume of hazardous

*Corresponding author.

sludge that becomes a problem for disposal. Each technique has its own advantages and disadvantages. A combination of these processes provides efficient treatment of dyeing effluent but at higher cost. Combination of electrochemical treatment and chemical coagulation [11], integration of chemical coagulation, electrochemical oxidation, activated sludge process [12], chemical oxidation with ozone [2], electrocoagulation [13] and combination of electrochemical method, chemical coagulation and ion exchange [14] were reported for treatment of textile effluent. The selection of the method mainly depends on the treatment target to be achieved.

Fluctuating concentration and flow rates make the conventional processes quite insufficient for the treatment of textile wastewaters, especially for colour removal [15,16]. Biological treatment though effectively reduces the biological and chemical oxygen demand (BOD and COD) of wastewater; it fails to decolorize the water completely. However, these methods are chemical intensive, time-consuming and require more operational cost.

Membrane-based separation processes, mainly nanofiltration, offer an attractive alternative in this regard that can be employed to remove the dyes and recovery of salts effectively. Membrane based technologies are cost-effective, energy efficient and treated water can be recycled. Nanofiltration and reverse osmosis are widely reported for dye removal [17,18]. Membrane fouling, however, is one of the major drawbacks of membrane technologies, since it causes decline of process throughput and deteriorates selectivity. Membrane performance is affected by operating conditions such as transmembrane pressure (TMP), cross-flow rate and feed characteristics. Therefore, the membrane processes are quite efficient in separation of dye but with associated operational problems, they are unable to handle large volume of effluent.

The present study aims to develop a hybrid separation scheme to decolorize the synthetic solution of reactive dye used in textile industries. The process involves two steps. In the first step, the dye is adsorbed onto activated carbon and in the second step, a multichannel ceramic microfiltration (MF) membrane is used to separate the dye-loaded activated carbon particles, operating at high throughput. The adsorption isotherm of various reactive dyes on activated carbon and effects of various operating conditions, such as pH, electrolyte solution and concentration of dye are studied in detail. Efficacy of MF is evaluated for separation of dye-loaded activated carbon by examining the effects of operating conditions, such as TMP drop and cross-flow velocity.

2. Experimental

2.1. Materials

Four commercial reactive dyes, yellow 15, black 5, red 24 and brown 10 were supplied by Central Glass and Ceramic Research Institute, Kolkata, India. Activated carbon, hydrochloric acid (HCl) and sodium hydroxide (NaOH) were procured from M/s Merck Specialities Pvt. Ltd., Mumbai, India.

2.2. Characterization of dye and prediction of the molecular size using molecular simulation

Chemical structure, molecular weight, molecular volume and wavelength at which maximum absorption of light for the dyes occur (λ_{max}) are presented in Table 1 [19–22]. The standard all atom CHARMM General Force Field parameters were applied for water and reactive dye molecules [23]. The topology and force field parameters for the dye molecules compatible with CHARMM were obtained using the formulation by Zoete et al. [24]. A single dye molecule was placed in the centre of 30 × 30 × 30 Å cubic box containing 1,000 water molecules. Van der waals interactions were based on Lennard Jones (L-J) 6–12 potential and the electrostatics via columbic interaction [25]. The molecular dynamic simulations were performed with the help of parallel architecture using 16 cores by utilization of the CHARMM v35b6 package [26].

2.3. Studies on adsorption

2.3.1. Adsorption isotherm

Equilibrium adsorption of activated carbon was determined by taking a fixed weight (0.2 g) of activated carbon in a series of synthetic dye solution of 200 mL each in Erlenmeyer flasks, with concentration varying from 1 to 1,200 mg/L for all four reactive dyes. pH of the solution was maintained at 4.5. The synthetic dye solution was kept in an orbital shaker with activated carbon at 150 rpm for 45 min. The temperature of the solution was maintained at 298 K for the equilibrium study. The amount of dye adsorbed on activated carbon was calculated by following mass balance equation,

$$Q_e = \frac{(C_0 - C_e) \times V}{W} \quad (1)$$

where Q_e is the amount of dye adsorbed per gram of activated carbon (mg/g); C_0 and C_e were the initial and equilibrium concentration of dye in water

Table 1
Chemical structure and physical properties of the reactive dyes

Dye	Chemical structure	λ_{max} (nm)	Molecular weight (g/mol)	Molecular volume (Å^3)
Reactive yellow 15	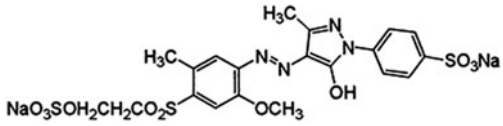	416	634.57	498
Reactive black 5	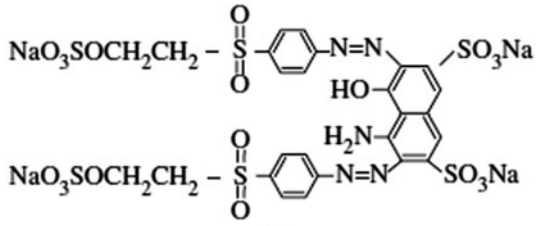	596	991.82	578
Reactive red 24	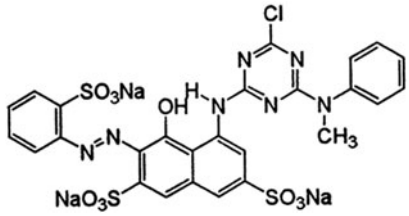	531	808.48	667
Reactive brown 10	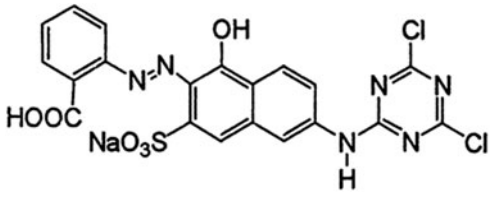	405	557.30	798

(mg/L); V is the volume of solution (L) and W is the weight of activated carbon (g).

2.3.2. Effect of pH and electrolytes on adsorption of dyes

The effect of pH of the feed solution and electrolyte concentration on the efficiency of adsorption was investigated. pH of the feed was varied from 2 to 11 using HCl and NaOH. Two hundred millilitre of synthetic dye solution was prepared using a dye concentration of 50 mg/L each. To each dye solution, 0.2 g of activated carbon was mixed and it was stirred in an orbital shaker at 150 rpm for 30 min at room temperature. The percentage adsorption was calculated by measuring absorption of dye using a UV–vis spectrophotometer supplied by M/s, Perkin Elmer, Connecticut, USA.

To study the effect of electrolyte concentration, three concentrations of sodium chloride were used in synthetic dye solutions of 50 mg/L of dye. These concentrations were 80, 100 and 120 g/L in three different batches. To each dye solution, 0.2 g of activated carbon was mixed and it was stirred in an orbital shaker at 150 rpm for 30 min at room temperature. Then the percentage adsorption was estimated.

2.3.3. Effect of adsorbent dose on dye removal

The effect of adsorbent dose on dye removal had been conducted in a series of experiments with all four reactive dyes. The adsorbent (activated carbon) dose was varied from 0.2 to 3 g/L for synthetic feed solutions of dyes at 50 and 150 mg/L. The pH was maintained at 4.5.

2.4. Hybrid filtration including adsorption followed by MF

2.4.1. Membrane module

A multichannel ceramic membrane module supplied by Central Glass & Ceramic Research Institute, Kolkata, India, was used in the experiments. The specifications of the membrane are presented in Table 2.

Table 2
Specifications of membrane

Item	Description
Type	Tubular multichannel module
Composition	Alumina-clay
Permeability of nascent membrane	1.44×10^{-3} L/m^2 h Pa
Length	20×10^{-2} m
Diameter of the module	3×10^{-2} m
Shape of the channels	Cylindrical
Number of channels	19
Channel diameter	4×10^{-3} m
Effective filtration area	4.75×10^{-2} m^2
Range of operating pH	1–14

2.4.2. Operating conditions of MF

Two concentrations, 50 and 150 mg/L of reactive dyes were used with 1 g/L of activated carbon at pH 4.5. MF experiments were carried out at different TMP (35, 69, and 104 kPa) and feed flow rates (50, 75, and 100 L/h) to determine the effect of operating conditions on permeate flux under total recycle mode. The TMP range was typical operating pressure in a MF process. The range of feed flow rate was selected to maintain the laminar flow. In batch mode of operation, the TMP was kept at 104 kPa and cross-flow rate was kept at 100 L/h.

2.4.3. Experimental set-up and the procedure

The schematic of cross-flow MF ceramic membrane set-up is shown in Fig. 1. The synthetic dye solution along with adsorbent particles was put in the feed tank. pH of the solution was maintained at 4.5. Mild stirring was provided at 100 rpm for 15 min. The reciprocating pump was then started to draw the solution from the feed tank to the membrane module. In this process, both valves at inlet and outlet of wash line were closed. The retentate was recycled back to the feed tank. The cross-flow velocity and the TMP drop were set operating the pump bypass valve and the retentate valve. Experiments were carried out in two different modes, total recycle mode and batch mode. In total recycle mode, the permeate was recycled back into the feed tank to maintain the uniform feed concentration. In case of batch mode, the permeate was drawn out constantly. The permeate flow rate was monitored continuously with the rotameter in the permeate line. Duration of the experiments with total recycle mode was 1 h and that the batch mode was 2.5 h. After the experiment, the feed tank was filled with tap water and cleaning protocol (as detailed in next section) was initiated. In the set-up, provision of backwashing was available.

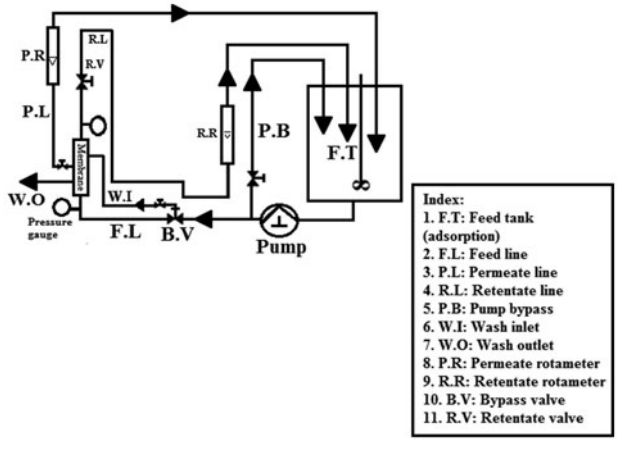

Fig. 1. Experimental set-up for hybrid separation process.

2.4.4. Membrane cleaning

To identify the efficient washing procedure, five different protocols were tested.

(1) Forward washing with stepwise increase in cross-flow rate (P1)

After the dye experiment (50 mg/L reactive brown dye, 1 g/L activated carbon) for 1 h, tap water was pumped through membrane module, keeping the inlet and outlet valves of wash line closed. At a particular TMP, cross-flow rate was increased from 25 to 100 L/h with a step of 25 L/h. Every step of the cross-flow rate was continued for 30 min. Two sets of TMP of 69 and 104 kPa were used.

(2) Backward washing with stepwise increase in cross-flow rate (P2)

After the experiment with activated carbon and dye solution, tap water was pumped through the wash line, closing the bypass (BV, in Fig. 1) and retentate valve (RV, in Fig. 1), with a circulation flow rate 25 L/h. The flow rate was increased to 100 L/h with a step of 25 L/h. Duration of each step was 30 min and the total washing period was 120 min.

(3) Forward washing of different durations (P3)

After a dye run of 50 mg/L reactive brown dye and 1 g/L activated carbon, forward washing using tap water at 120 kPa and 100 L/h cross-flow rate was used for 15 min. Then the same feed solution was filtered for 50 min. Next, the forward washing was continued for 30 min under the same operating conditions. Again MF was conducted for 50 min followed by forward washing for 45 min. Likewise, the duration of the last forward washing was 60 min.

(4) Backward washing of different duration (P4)

After MF of feed solution (50 mg/L reactive brown dye with 1 g/L activated carbon), backward washing using tap water was conducted at 100 L/h for different durations, e.g. 15, 30, 45 and 60 min. The sequence of experiments was MF followed by backward washing of different duration as described in the preceding protocol (P3).

(5) Acid–alkali washing (P5)

After the dye run is over, the inlet and outlet valves of the washing line were closed and tap water was pumped for 2 min to clear out any loose activated carbon particle. Then 1 (N) HCl was recycled within the set-up for around 30 min at 120 kPa and 100 L/h, followed by 1 (N) NaOH for 30 min in the same operating condition. Then the set-up was thoroughly rinsed with tap water for around 1 h. The pH of the permeate line was occasionally monitored during the end of the tap water washing to ensure a neutral pH in the lines.

2.5. Analysis

2.5.1. Characterization of activated carbon

2.5.1.1. Particle size analysis for activated carbon. The particle size for activated carbon was measured using Mastersizer 2000, Malvern instruments, Worcestershire, England.

2.5.1.2. Determination of pore size. The pore size of the ceramic membrane was measured by Mercury Intrusion Porometer PM60, Quantachrome, Florida, USA.

2.5.2. Characterization of membrane

2.5.2.1. Permeability. The hydraulic permeability of the membrane was determined by measuring the permeate flux using distilled water at different TMP 35, 69, 104 and 138 kPa, respectively, keeping the flow rate same in each case. A plot of flux against TMP drop results in a straight line passing through the origin, the slope of which gives the hydraulic permeability. The initial permeability of the ceramic membrane was found to be 1.44×10^{-3} L/m^2 h Pa as shown in Fig. 2.

2.5.3. Measurement of dye concentration and other parameters

Dye concentration in any stream was measured using a UV–vis spectrophotometer supplied by M/s, Perkin Elmer, Connecticut, USA, at a wavelength where maximum absorbance occurs. The dye rejection was evaluated using the following relation:

$$R = \left[1 - \frac{C_p}{C_0}\right] \times 100\% \quad (2)$$

where C_P and C_0 are dye concentration in permeate and feed. pH, conductivity and total dissolved solids in feed and permeate were measured using a multi

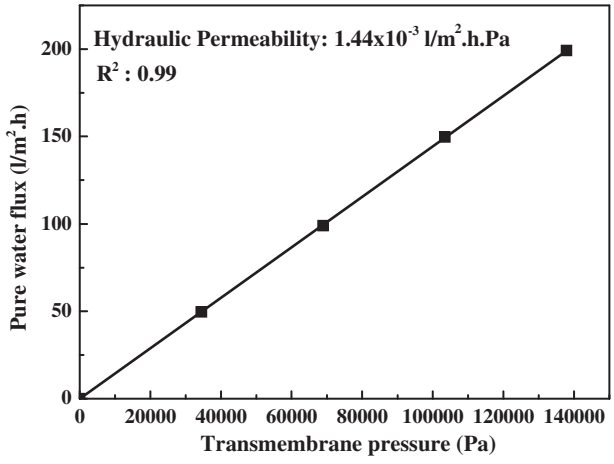

Fig. 2. Pure water flux with TMP for nascent membrane.

parameter pocket tester (EUTECH Instruments Ltd., Singapore).

3. Results and discussion

3.1. Adsorption

3.1.1. Characterization of adsorbent

3.1.1.1. Determination of particle size for activated carbon. The size distribution of activated carbon is shown in Fig. 3. It is observed from this figure that the average size of adsorbents is 14 μm with a range from 0.5 to 300 μm.

3.1.2. Adsorption Isotherm

Adsorption isotherm is the relationship between substance adsorbed and its concentration in equilibrium solution at constant temperature [27]. Two standard isotherms, namely, Langmuir and Freundlich are utilized to explain the adsorption behaviour. These are the most widely used adsorption isotherms to characterize the dye adsorption property on activated carbon. Fitting of other isotherms for adsorption of reactive dyes on activated carbon is also available in the literature [28–31]. The linearized form of Langmuir isotherm is shown in Eq. (3).

$$\frac{C_e}{Q_e} = \frac{C_e}{Q_m} + \frac{1}{KQ_m} \tag{3}$$

where C_e is equilibrium concentration of dye in the solution (mg/L); Q_e is amount of dye adsorbed per unit mass of adsorbent (mg/g); Q_m is adsorption capacity (mg/g) and K is adsorption equilibrium constant (L/mg). Similarly, the log-linear form of Freundlich isotherm is

$$\log Q_e = \frac{1}{n}\log C_e + \log K_f \tag{4}$$

where n and K_f ($mgL^{-1/n}\,L^{1/n}\,g^{-1}$) are Freundlich constants. The linear forms of Eqs. (3) and (4) corresponding to all dyes are presented in Fig. 4(a) and (b) for Langmuir and Freundlich isotherms, respectively. The values of evaluated constants for different dyes are tabulated in Table 3. As evident from this table, Langmuir isotherm fits the experimental data better than Freundlich isotherm due to much higher values of correlation coefficient. Therefore, dye adsorption occurs homogeneously in monolayer, i.e. adsorption occurs at specific sites on the adsorbent and once the site is occupied by one dye molecule further adsorption will not occur there. Maximum Langmuir adsorption capacity for these dyes is as follows: 152 mg/g for reactive brown; 147 mg/g for reactive yellow; 135 mg/g for reactive red and 130 mg/g for reactive black. Another measure of adsorption efficiency is separation factor (RL). It is defined as,

$$R_L = \frac{1}{1 + KC_0} \tag{5}$$

where K is Langmuir constant and C_0 is initial feed concentration. RL < 1 indicates favourable adsorption. As observed from Table 4, for all the dyes with the concentration in the experimental range, the adsorption is highly favourable.

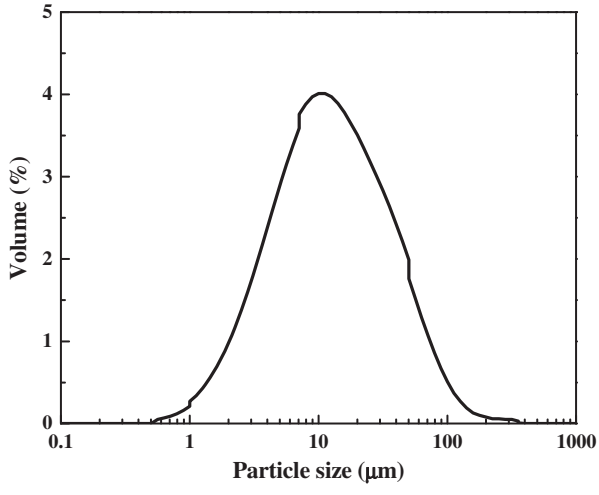

Fig. 3. Particle size analysis for activated carbon.

3.1.3. Adsorption kinetics

The kinetic study was conducted for all four dyes and the results are presented in Fig. 5. It is observed from this figure that the dye concentration decreases sharply and beyond 30 min the change in concentration is marginal.

3.1.4. Effect of pH and salt concentration on adsorption of reactive dyes

Effects of pH and salt concentration on adsorption of reactive dyes are presented in Fig. 6(a) and (b), respectively. It is evident from Fig. 6(a) that maximum adsorption occurs at lower pH in the range 2–5. Extent of adsorption in this pH range is also uniform. This result is in accordance with the observations reported

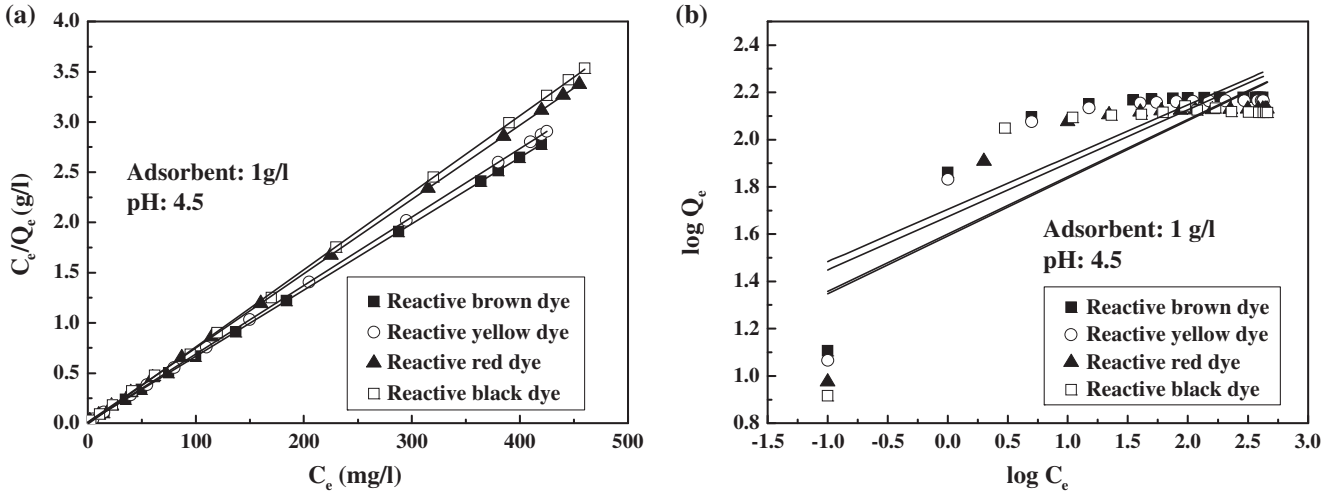

Fig. 4. (a) Langmuir isotherm and (b) Freundlich isotherm plot for dye adsorption.

Table 3
Values of Langmuir and Freundlich isotherm constants

	Langmuir constants			Freundlich constants			
Dye	K (L/mg)	Q_m (mg/g)	R^2	K_f ($mg^{1-1/n}\ L^{1/n}\ g^{-1}$)	n	R^2	Separation factor (R_L)
Reactive yellow dye	0.92	152	0.99	50.7	4.5	0.68	0.001–0.1
Reactive brown dye	0.85	147	1.0	47.2	4.4	0.69	0.001–0.11
Reactive red dye	0.77	135	1.0	39.8	4.1	0.68	0.001–0.12
Reactive black dye	0.67	130	0.99	39.1	4.1	0.61	0.0012–0.13

Table 4
Composition of the ceramic membrane

Compound name	Weight percentage
Calcium carbonate ($CaCO_3$)	35.31
Silicon dioxide (SiO_2)	45.64
Aluminium oxide (Al_2O_3)	19.05

by Al-Degs et al. [31]. Value of pH_{ZPC} of commercial activated carbon is 9.0 [31] and pKa values of the reactive dyes are in the range of 4.4–5.5 [31]. At lower pH, the sulphonate groups of the dyes were protonated making it $–SO_3H$, which makes the dye solution almost neutral or slightly positive. Therefore, it is likely that electrostatic interaction dictates repulsion or marginal interaction between the dye molecules and positively charged adsorbent surface, resulting in lower adsorption. On the other hand, in this pH range, the adsorption is maximum and close to 100%. This clearly indicates that electrostatic interaction is not the sole mechanism of facilitation of adsorption of reactive dyes on the activated carbon surface. Strong

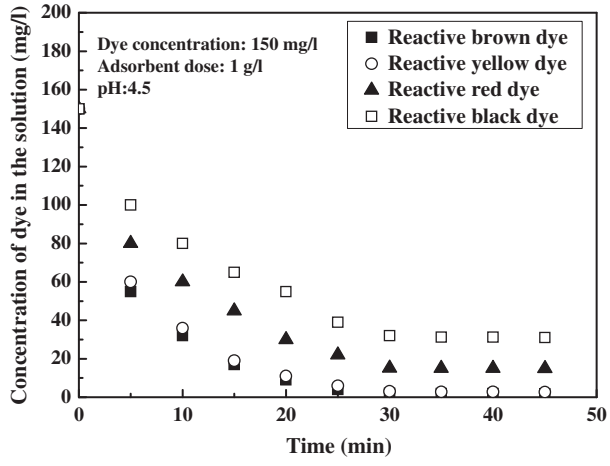

Fig. 5. Adsorption kinetics for reactive dyes at a feed concentration of 150 mg/L.

hydrogen bonding between the dyes and carbon surface and hydrophobic interaction between them may be the reason of enhanced adsorption at lower pH

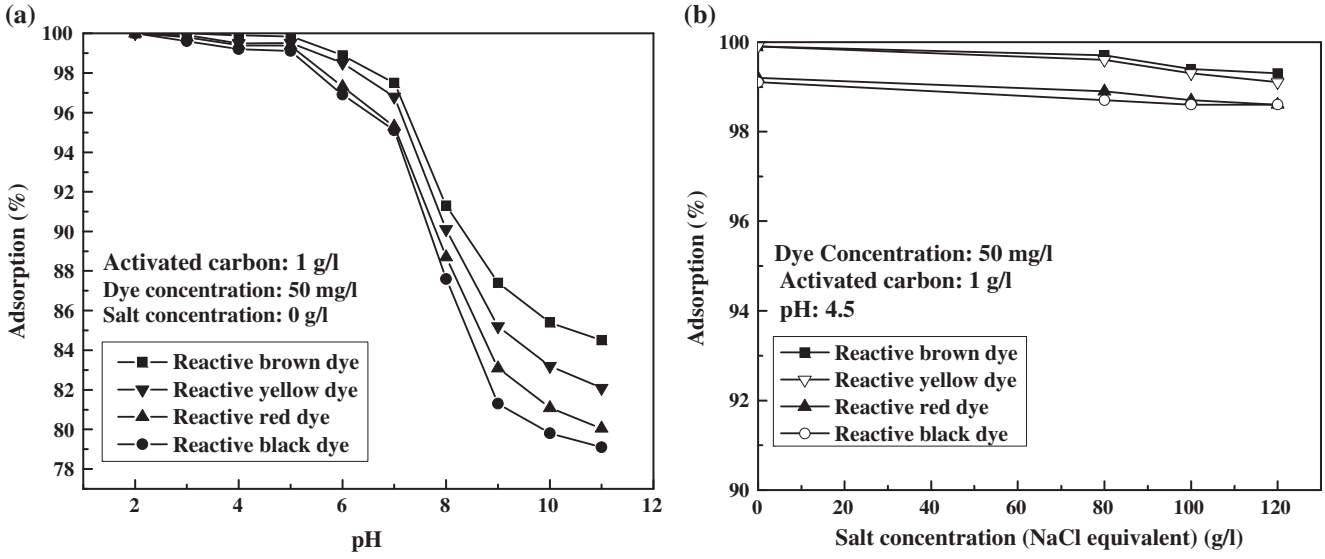

Fig. 6. Effect of (a) pH and (b) salt concentration on adsorption of reactive dyes on activated carbon.

range [31–33]. At higher pH above 9, both dye molecules and the adsorbent possess negative charge and electrostatic repulsion plays an important role, leading to lower adsorption. At pH 11, the adsorption of various dyes is in the range of 80–85%. This also confirms that electrostatic interaction is not the sole mechanism of adsorption. In between pH 4 and 6, the dye molecules are practically neutral, and hence their adsorption onto the carbon surface (positively charged) is not facilitated by electrostatic interactions, thereby decreasing the extent of adsorption.

From Fig. 6(b), it can be seen that with increase in salt concentration in the feed, the adsorption of reactive dye decreases marginally at pH 4.5. At this pH, the adsorbent is positively charged and the dye molecules are almost neutral. Therefore, there is a competitive adsorption between the negatively charged chloride ions and almost neutral dye molecules. However, chloride ions being much smaller in size, this phenomenon leads to slight decrease in dye adsorption. With the increase in salt concentration from 80 to 120 g/L, the percentage decrease in adsorption of dyes by activated carbon is 0.5–0.8%, which is negligible.

3.2. Microfiltration

3.2.1. Composition of the ceramic membrane

The EDX of the ceramic membrane reveals its composition and these are shown in Table 4. This table indicates that silica content is maximum followed by calcium carbonate and alumina.

3.2.2. Pore size of ceramic membrane

The pore size of the ceramic membrane was measured by Mercury Intrusion Porometer, and it was found out to be 0.2 μm. Pore size distribution of the membrane was presented in Fig. 7.

3.2.3. Cross-flow MF under total recycle mode

In total recycle mode, both the retentate and permeate are recycled to the feed tank to make the feed concentration uniform. Fig. 8(a)–(d) represent the permeate flux profiles corresponding to different dye solution having initial concentration of 50 mg/L

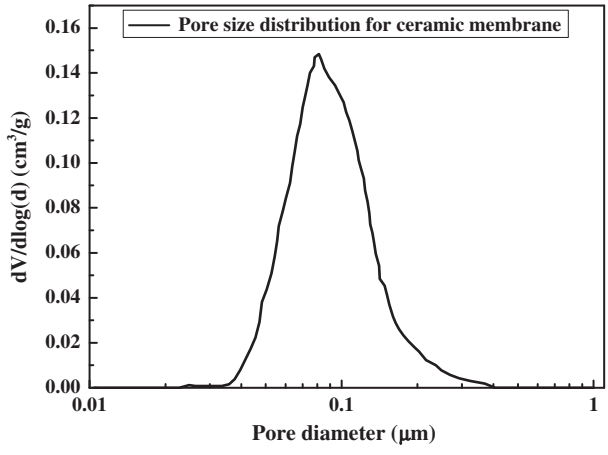

Fig. 7. Differential pore size distribution for ceramic membrane.

(before adsorption) with adsorbent dose 1 g/L at pH 4.5. Activated carbon particles, being larger in size (average diameter is 14 μm) compared to pore size of the membrane (0.2 μm), deposit on the membrane surface forming a cake type of layer almost at the start of the experiment. For example, at TMP at 104 kPa, the pure water flux was 150 L/m^2 h. At the same TMP, the measured flux at the beginning is 110 L/m^2 h for yellow dye, 95 L/m^2 h for black, 100 L/m^2 h for red and 128 L/m^2 h for brown reactive dye. These data confirm the instantaneous growth of cake layer of carbon particles on the membrane surface. These figures exhibit the expected trends that the permeate flux increases with TMP due to increase in driving force and with cross-flow velocity due to increase in the shearing effect imposed by forced convection induced by feed cross-flow. For example, in case of reactive yellow dye, at 35 kPa TMP, the steady-state flux is 40 L/m^2 h at a flow rate of 50 L/h and that for 69 and 104 kPa is 56 and 88 L/m^2 h, respectively at the same cross-flow rate. Thus, the increment in steady-state flux is around 40% for 69 kPa and 120% for 104 kPa (compared to TMP 35 kPa). Similar trends are observed for other dyes. These data clearly confirm that within the range of TMP used in this study, the filtration is not pressure independent. Pressure-independent cake filtration may occur at higher TMP. Also with the increase in cross-flow rate from 50 to 100 L/h, the increment in permeate flux is around 15, 11 and 15%, for 35, 69 and 104 kPa, respectively. However, the axial pressure drop was in the range of 7–10 kPa only for the cross-flow rates considered herein. This shows improvement in mass transfer with cross-flow and reduction in the cake layer resistance against the solvent flux.

From Fig. 8(b), it is also observed that the permeate flux for reactive black dye is the lowest among all the dyes corresponding to identical set of operating conditions. This is because, the molecular size of reactive black dye is the highest among the dyes, as evident from their molecular weight and volume as shown in Table 1. Thus, the effective size of the adsorbent particles loaded with the adsorbed dyes is more for reactive black, leading to enhanced thickness of the cake layer, thereby lowering the permeate flux. For example, at 104 kPa TMP and 100 L/h cross-flow

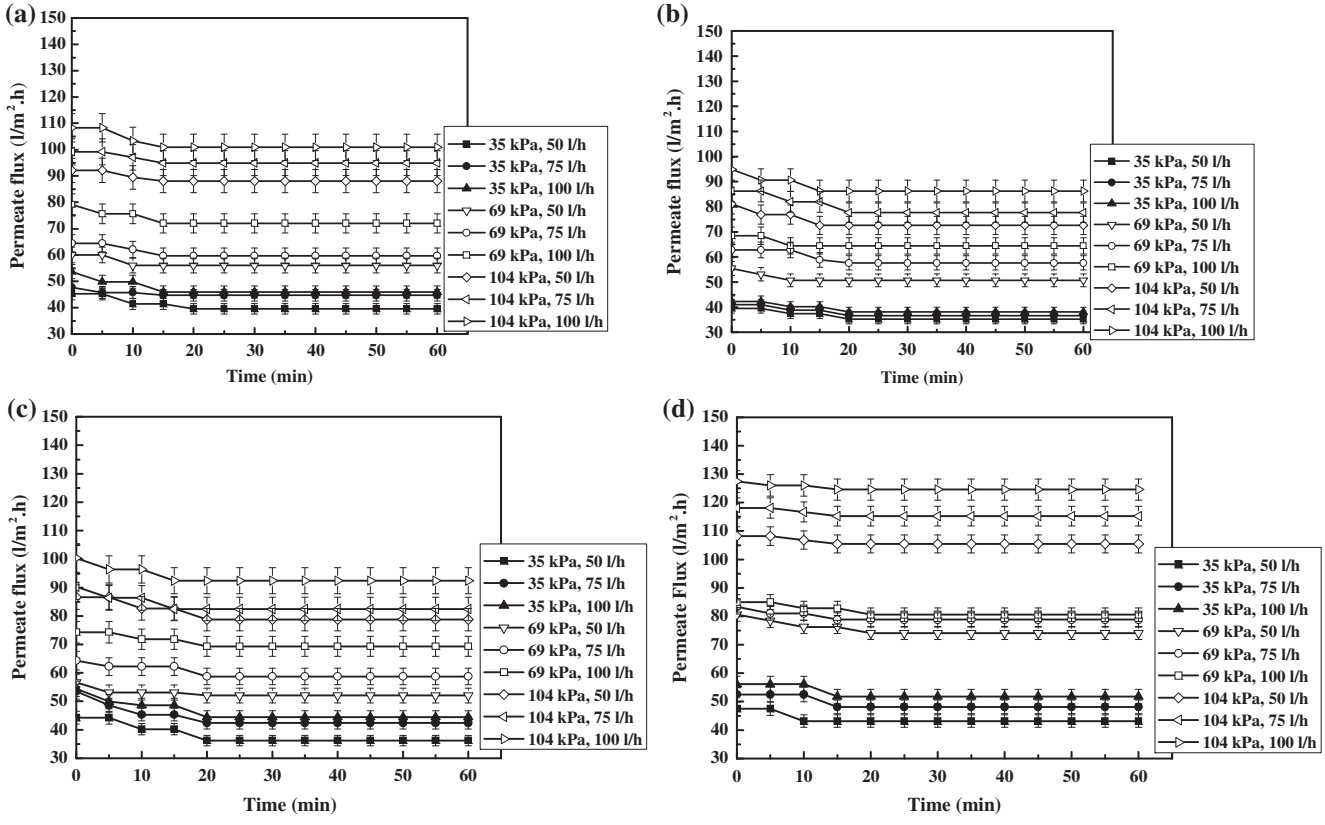

Fig. 8. Profiles of permeate flux under cross-flow recycle mode (dye concentration, 50 mg/L). (a) Reactive yellow dye, (b) reactive black dye, (c) reactive red dye, and (d) reactive brown dye.

rate, the steady-state permeate flux is 90 L/m^2 h for reactive black. Under the same operating conditions, the permeate flux is 105, 95 and 125 L/m^2 h for reactive yellow, red and brown dyes. The trend is similar for other operating conditions.

As observed in Fig. 8(c), the steady-state flux for reactive red under all operating conditions is less than that of reactive yellow but more than that of reactive black. The variation of flux values is marginal. This is due to the difference in molecular sizes of the dyes (refer Table 1 for the molecular weight and volume of dyes). Increasing cross-flow rate from 50 to 100 L/h, the permeate flux increases from 36 to 44 L/m^2 h (22%) at 35 kPa; 52–69 L/m^2 h (33%) at 69 kPa and 79–92 L/m^2 h (16%) at 104 kPa. The enhancement of permeate flux with cross-flow rate is due to the reduction of thickness of cake layer at higher cross-flow rate, imparting more shear force on cake layer as described earlier. At higher TMP, the enhancement due to increase in cross-flow rate of identical magnitude, leads to reduced increment (16% compared to 33%) indicating that the cake layer becomes more compact imparting extra resistance to the permeation of the solvent at higher TMP. In Fig. 8(d), the flux profiles of reactive brown are presented. The permeate flux for reactive brown is the highest among four dyes. The molecular size of this dye is the lowest (refer Table 1).

The permeate flux profiles of various dyes are shown in Fig. 9 at dye concentration 150 mg/L (before adsorption). At enhanced feed concentration, additional dye particles are adhered to the surface of activated carbon making it more bulky, offering more resistance to the solvent flux during its passage through cake layer formed by adsorbents. This leads to decrease in permeate flux compared to that at 50 mg/L dye concentration before adsorption under all operating conditions as shown in Fig. 8. However, since the particle size of the dyes is quite small compared to that of activated carbon, the decrease in flux is marginal. For example, at 104 kPa TMP and 100 L/h cross-flow rate, the steady-state permeate flux of reactive yellow is 100 L/m^2 h at 50 mg/L dye concentration before adsorption. Under the same operating conditions, the permeate flux is reduced to 94 L/m^2 h at 150 mg/L dye concentration before adsorption. This trend is similar for all other operating conditions for all dyes.

3.2.4. Effect of adsorbent dose on dye removal

In the adsorption–MF hybrid process, the dyes are removed in the adsorption step and dye-loaded adsorbents are removed by MF. Thus, the removal of dyes occurs in the first step itself, and hence their removal is independent of the operating conditions of MF.

However, adsorbent dose plays an important role in dye removal. Removal of all dyes is more than 99% at 50 mg/L feed concentration at 1 g/L dose of adsorbent as shown in Fig. 10(a). Under the same loading of adsorbent, the removal of dyes at feed concentration 150 mg/L (before adsorption) is more than 99% except reactive black (79–80%) and red (85–86%). The molecular weight and hence the size of reactive black and red are the highest (991 and 808 g/mol, respectively, in Table 1) among the four dyes. Thus, less number of dye particles at higher concentration (150 mg/L) is adsorbed on the adsorbent compared to those corresponding to 50 mg/L as shown in Fig. 10(b). On the other hand, for other dyes with molecular weight less than that of reactive yellow (molecular weight 634 g/mol), the size of the dye molecules are such that even at 150 mg/L feed concentration, the adsorption is complete. However, the trial runs indicate that slight increase in adsorbent dose to 1.5 g/L leads to complete removal of these two reactive dyes even at concentration 150 mg/L as evident from Fig. 10(b). The other quality parameters of the feed are pH 4.2, conductivity 106.3 mS/cm, total dissolved solids 72.5 g/L. These values for the permeate are 4.2, 44 mS/cm and 31 g/L, respectively.

3.2.5. Cross-flow MF under batch mode

In the batch mode, the permeate is not recycled back to the feed tank. As a result, the feed concentration increases due to the decrease in feed volume during filtration. The volume concentration factor, VCF ($\frac{V_0}{V^t}$ where V_0 is defined as the initial feed volume and V^t is defined as the volume of the feed after a certain time 't') increases with time. Since the feed concentration increases in time, the permeate flux never attains a steady state under the batch mode. The profiles of permeate flux for all the dyes at 50 mg/L feed concentration and at 1 g/L adsorbent dose are shown in Fig. 11. The striking feature of this figure compared to that under total recycle mode (Fig. 8) is the flux decline is more prominent in this case. The decline is sharp upto 50 min for reactive black and it is upto 20 min for reactive brown. As the filtration progresses, the concentration of solutes (adsorbents) increases in the feed, resulting in more deposition of them on the membrane surface, leading to a thicker cake layer. Since the cake layer grows in time, the resistance against the solvent flux also increases and finally permeate flux declines to a substantial extent. For

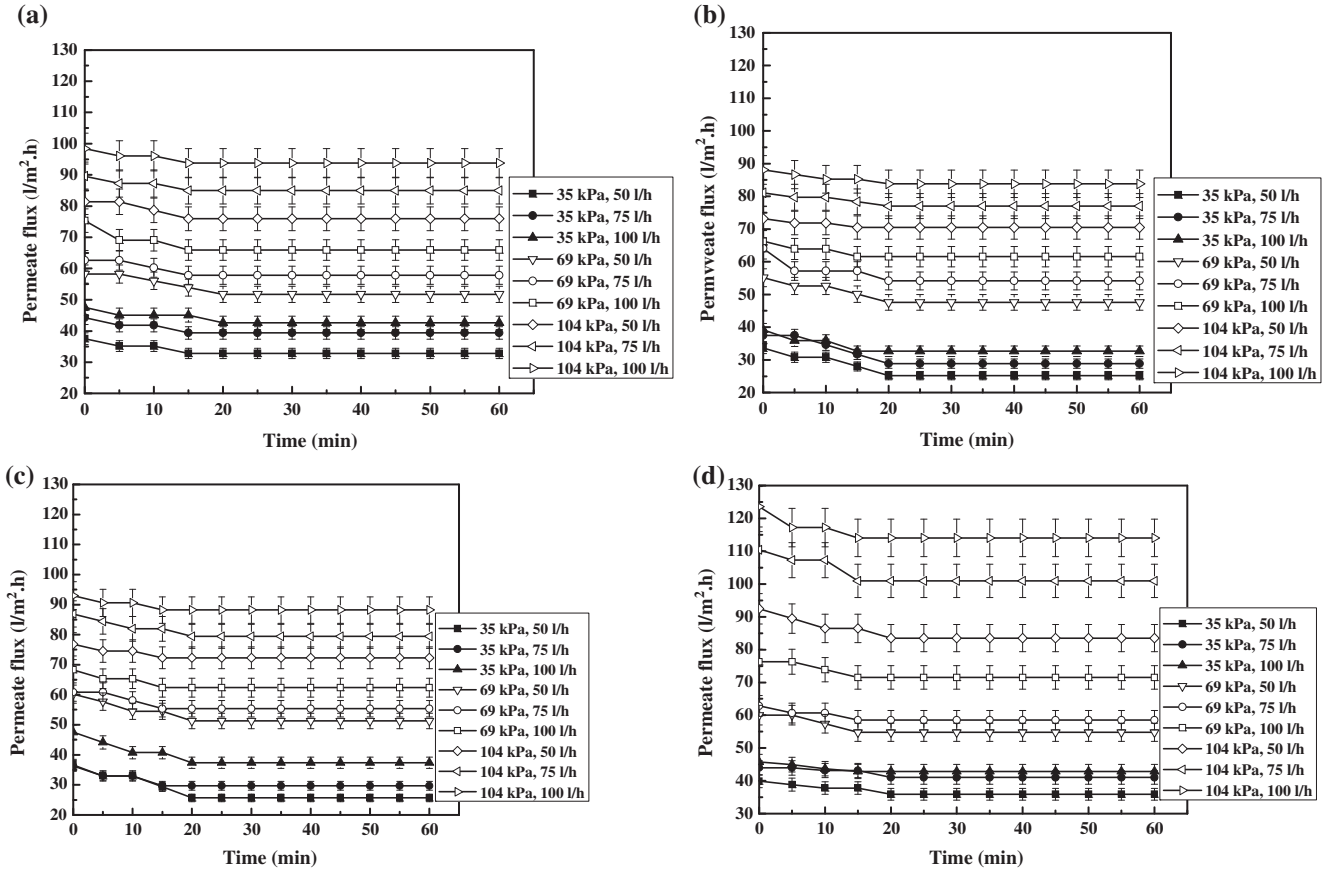

Fig. 9. Profiles of permeate flux under cross-flow recycle mode (dye concentration, 150 mg/L). (a) Reactive yellow dye, (b) reactive black dye, (c) reactive red dye, and (d) reactive brown dye.

example, in case of reactive black, the permeate flux declines by about 20% (127–103 L/m^2 h) within 140 min. However, the profiles of flux decline for different dyes reveal an interesting trend. Permeate flux decline is steeper in case of dyes of higher molecular weight. Flux decline for reactive brown having the lowest molecular weight (557) has the most gradual decline (from 127 to 120 L/m^2 h in 120 min). This observation is in corroboration with the interaction between dye molecules and the adsorbent as discussed in Section 3.2.3. Bulkier dyes (higher molecular weight) make the adsorbent–dye agglomerate larger in size, thereby forming a thicker cake layer, and hence the flux decline is more. Flux decline is greater for reactive black > red > yellow > black in that order and the molecular weight and volume of the dyes also decreases in the same order (refer Table 1).

A profile of VCF and bulk concentration of activated carbon is presented in Fig. 12. It was observed from this figure that VCF attains the value 3.3 within 2.5 h of operation in batch mode. At the same time, the bulk concentration also increases upto three times the initial feed concentration. Similar trends (including numerical values) are observed for other dyes. This is due to the fact that the adsorbent particles are mainly filtered in MF.

3.3. Effect of different washing conditions

3.3.1. Forward washing with stepwise increase in cross-flow rate (P1)

A solution of 50 mg/L reactive brown with 1 g/L activated carbon was filtered at 69 kPa TMP and 25 L/h cross flow rate under total recycle mode for 30 min. Tap water was pumped into the system (closing wash line valves) at 69 kPa and 25 L/h cross-flow rate. The cross-flow rate is increased in step of 25 L/h till 100 L/h with each cross-flow of 30 min, duration as explained in Section 2.4.4. The profile of water flux during the complete duration of 120 min (4 cross flow of 30 min each) is shown in Fig. 13. The procedure is repeated at a higher TMP, 104 kPa and the results are also shown in the same figure. From Fig. 13, it has been observed that by

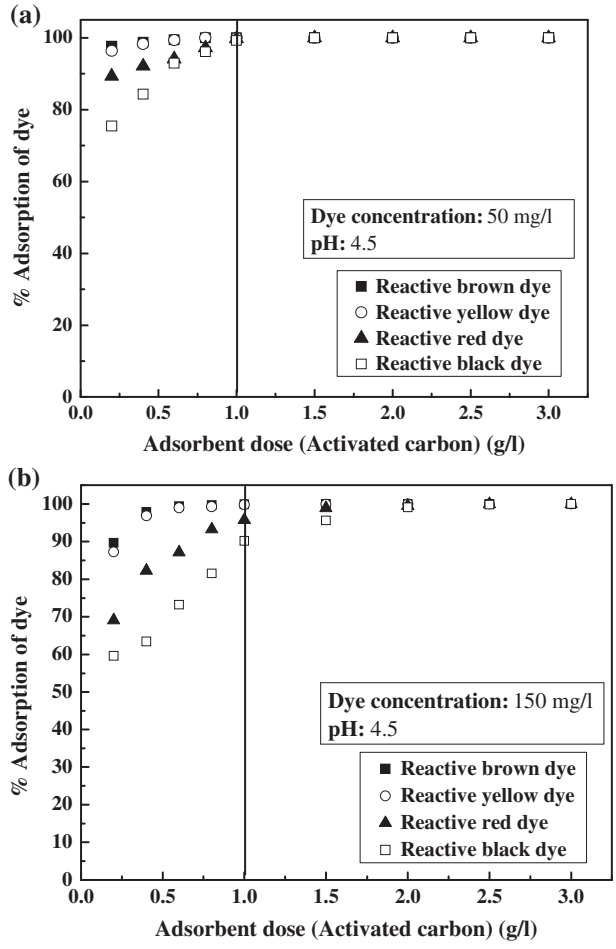

Fig. 10. Percentage adsorption of (a) 50 mg/L and (b) 150 mg/L of reactive dyes with adsorbent dose.

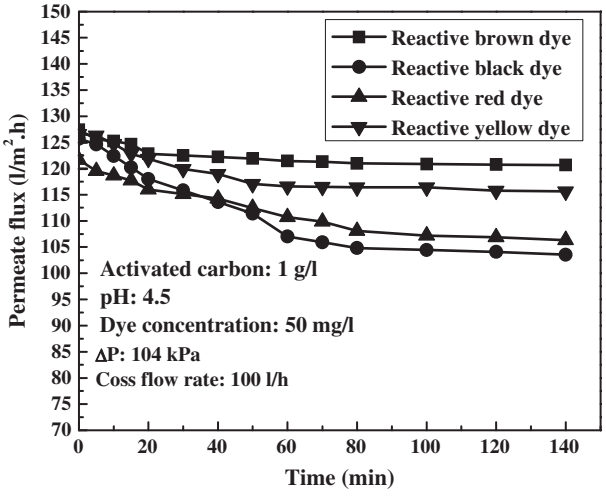

Fig. 11. Profiles of permeate flux under batch mode of cross-flow filtration.

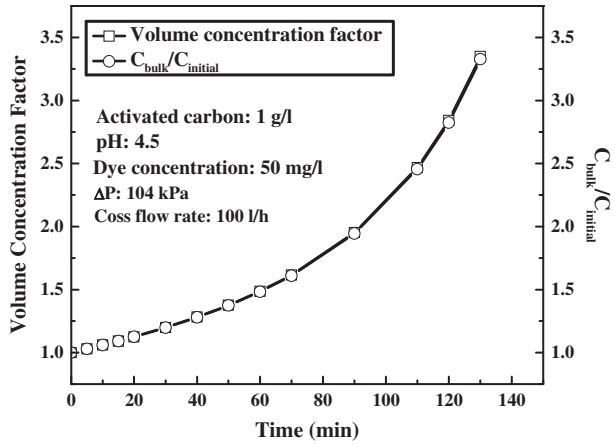

Fig. 12. Volume concentration factor and change in bulk concentration for reactive yellow dye under batch mode of cross-flow filtration.

this procedure the maximum water flux that can be achieved is 77 L/m^2 h for 69 kPa and 130 L/m^2 h for 104 kPa. It may be noted that pure water flux for the clean membrane is 100 and 150 L/m^2 h at 69 and 104 kPa TMP. This study indicates that higher TMP and cross-flow rate in P1 mode of cleaning favour recovery of membrane permeability.

3.3.2. *Backward washing with stepwise increase in cross-flow rate (P2)*

The procedure of backwashing is presented in Section 2.4.4. In short, after a dye experiment (50 mg/L reactive brown; 1 g/L activated carbon; 69 kPa TMP; 25 L/h cross-flow rate under total recycle mode for 30 min), backwashing was carried out at 25 L/h under normal atmospheric pressure with tap water. After

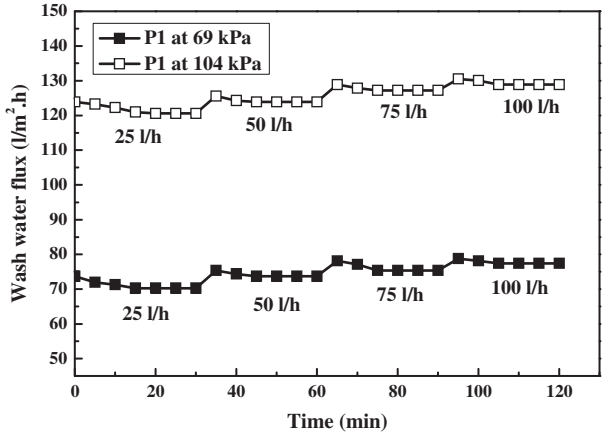

Fig. 13. Performance of washing protocol P1.

30 min, the circulation rate was enhanced stepwise to 100 L/h with a step of 25 L/h. Duration of each step was 30 min. At the end of washing cycle, i.e. 120 min (four flow rates of 30 min each), the membrane permeability was measured. The permeability after backwashing was 1.27×10^{-3} L/m^2 h Pa compared to 1.44×10^{-3} L/m^2 h Pa, indicating about 88% recovery of membrane permeability.

3.3.3. Forward and backward washing of different durations (P3 and P4)

The details of these protocols are presented in Section 2.4.4. In this case, the sequence of experiments was: (i) dye experiment for 50 min; (ii) cleaning by tap water for 15 min; (iii) dye experiment for 50 min; (iv) cleaning by tap water for 30 min; (v) dye experiment for 50 min; (vi) cleaning by tap water for 45 min; (vii) dye experiment for 50 min; and (viii) cleaning by tap water for 60 min. In case of forward washing, the operating conditions were 120 kPa TMP and 100 L/h cross-flow rate. For backward washing, the circulation rate was 100 L/h at atmospheric pressure. Membrane permeability after each washing step was measured for both the cases and the results are shown in Fig. 14. It is observed from this figure that washing protocol P4 performs better than P3. In case of P3, membrane permeability decreases monotonically and after four washing, it is 1.01×10^{-3} L/m^2 h Pa compared to 1.44×10^{-3} L/m^2 h Pa of nascent membrane. On the other hand, in case of P4, the efficiency of backwashing is clearly demonstrated. After backwashing of 15 min, the permeability decreases to 1.22 × 10−3 L/m^2 h Pa and after subsequent cleaning of longer duration, membrane permeability is recovered better. At the end of fourth backwashing, permeability was recovered to 1.33 × 10−3 L/m^2 h Pa which is about 93% of original permeability. For P4, backwashing is more effective to loosen up the particles in cake layer and wash them off.

3.3.4. Acid–alkali wash (P5)

This washing protocol is presented in Section 2.4.4. In this case, 100% recovery of permeability was attained. Higher efficiency of acid–alkali wash and the possible mechanisms are reported in the literature. Regeneration of activated carbon using acid wash was reported by Martin and Ng [34]. During acid treatment (at pH less than 2), both the activated carbon (pH_{ZPC} = 9.0) and dye molecules (pKa 4.4–5.5) are positively charged and the electrostatic repulsion takes place. This facilitates the physical dislodgement of

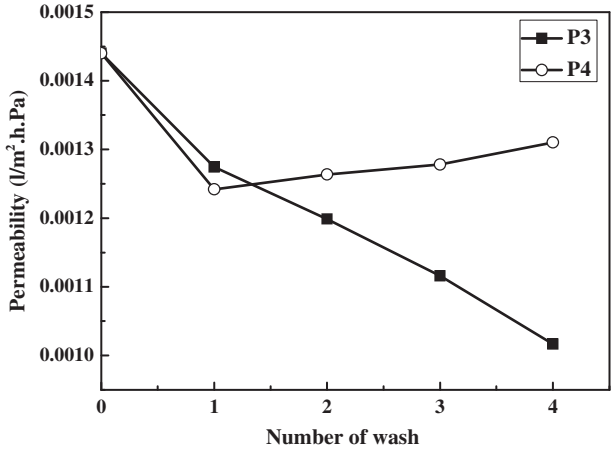

Fig. 14. Recovery of permeability for washing protocols P3 and P4.

dyes from activated carbon surface [31,34]. During alkali treatment (at pH 12), activated carbon becomes negatively charged and their solubility increases in alkaline solution [35,36], leading to their disintegration. Also, the negative functional groups of activated carbon repel each other under strong alkaline environment, leading to their dissolution [36]. Therefore, the cake layer is completely removed and under these mechanisms, even some smaller sized carbon particles blocking the inside pore of the membranes get dissolved. Therefore, acid–alkali treatment results 100% recovery of membrane permeability.

3.4. The comparison between this method and other methods for similar treatment of dyes and textile effluent

Comparison of performance between the present work and other hybrid and single-stage separation processes is presented in Table 5. Almost complete removal of reactive black and reactive orange was reported by a hybrid process consisting of adsorption, coagulation and submerged MF [37]. Similarly, coagulation/flocculation followed by submerged MF/ultrafiltration (UF) of dye from effluent resulted to 50–75% removal of dye [38]. Micellar-enhanced UF of reactive dyes (50–500 mg/L) and methylene blue (6 mg/L) resulted in high dye removal (>97%) [39–41]. Throughput of the process for reactive dye systems was quite low, 7×10^{-5}–9×10^{-5} L/m^2 h Pa. However, limitations of these processes involve recovery of surfactants and destabilization of micelles under high concentration of salts in actual textile effluent. Polyelectrolyte-enhanced nanofiltration is another hybrid process for removal of reactive

Table 5
Performance comparison between the present and reported hybrid/single separation systems

Serial No.	Hybrid/single separation system	Operating condition		Dye and feed concentration (mg/L)	Process throughput (L/m^2 h Pa)	Dye removal (%)	References
		Pressure (kPa)	Cross-flow rate (L/h)/ Reynolds number				
1	Adsorption + coagulation + submerged microfiltration. Polyethylene hollow fibre MF membrane	–	–	Reactive black and reactive orange 16 (250 mg/L)	–	99.9	[37]
2	Coagulation/Flocculation + submerged microfiltration/ultrafiltration polysulfone hollow fibre MF/UF membrane	10	15–25	Dyehouse effluent	–	50–74	[38]
3	Micellar-enhanced ultrafiltration (UF) using sodium dodecyl sulphate polysulfone hollow fibre UF membrane	10–90	–	Methylene blue (6 mg/L)	4.5×10^{-4}–1.3×10^{-3}	99	[39]
4	Micellar-enhanced ultrafiltration using Cetyl pyridium chloride Flat sheet batch UF membrane	300	–	Reactive black 5 and Reactive orange 16 (50 mg/L)	8×10^{-5}	97–99	[40]
5	Micellar-enhanced ultrafiltration using cetyl pyridium chloride Flat sheet batch UF membrane	300–500	–	Reactive black 5 (500 mg/L)	7×10^{-5}	98.82–97.39	[41]
				Reactive orange 16 (500 mg/L)	9×10^{-5}	99.79–99.05	
6	Nanofiltration(NF) polyamide flat sheet NF membrane	300–1,100	–	Textile effluent	1×10^{-5}–5×10^{-5}	>95	[42]
	Ultrafiltration + nanofiltration tubular ceramic UF membrane	300–1,300			2.5×10^{-5}–5×10^{-5}	>99	
7	Polyelectrolyte-enhanced nanofiltration flat sheet cross-flow NF polyelectrolyte membrane	480	1.08	Reactive orange 16, Reactive blue 4 and Reactive black 5 (1,000 mg/L)	1.5×10^{-4}–2.1×10^{-4}	99.9	[43]
8	Nanofiltration polysulfone–polyamide flat sheet NF membrane	800–2,400	Reynolds number 1,500–10,000	Reactive black 5 (1,000–50,000 mg/L)	3.5×10^{-5}–5×10^{-5}	99.8	[17]
				Reactive orange 16 (100 to 5,000 mg/L)	2.5×10^{-5}–3×10^{-5}		
9	Nanofiltration polyamide thin film composite NF membrane	1,000	Reynolds number up to 4,100	Direct red 80 (1,000 mg/L)	2.7×10^{-5}–4×10^{-5}	99–100	[44]
				Disperse blue 56 (1,000 mg/L)	3×10^{-5}–4×10^{-5}	99–100	
				Acid red 4 (1,000 mg/L)	1.3×10^{-5}–2×10^{-5}	83–96	
				Basic blue 3 (1,000 mg/L)	1.3×10^{-5}–2×10^{-5}	21–41	

10	Present work (adsorption of reactive dyes with activated carbon followed by ceramic microfiltration)	35–104	50 to 100	Reactive yellow 15 (50 mg/L) (150 mg/L)	9.7×10^{-4}–1.14×10^{-3}	>99 >98	This work
				Reactive black 5 (50 mg/L) (150 mg/L)	8.1×10^{-4}–1×10^{-3}	>98 80	
				Reactive red 24 (50 mg/L) (150 mg/L)	8.8×10^{-4}–1.02×10^{-3}	>99 85	
				Reactive brown 10 (50 mg/L) (150 mg/L)	1.2×10^{-3}–1.23×10^{-3}	>99 >99	

dyes [42]. However, recovery of polyelectrolytes from the retentate is another additional step that increases operating cost. This process also resulted in high dye removal (>99%), relatively higher throughput (1.5×10^{-4}–$2.1 \times 10{-}4$ L/m^2 h Pa) but the performance deteriorated at higher salt concentration in a textile effluent. For single-stage nanofiltration [17,43,44], although high dye removal (>99%) was reported, the throughput of the process was quite low (1.3×10^{-5}–5×10^{-5} L/m^2 h Pa). In the present work, at the first stage itself, complete dye removal was attained by adsorption (>99% for 50 mg/L of all dyes at 1 g/L adsorbent dose [Fig. 11(a)] and at 1.5 g/L for 150 mg/L dye concentration for reactive black and brown) [Fig. 11(b)]. The throughput of the system was high (8.1×10^{-4}–1.2×10^{-3} L/m^2 h Pa) and it was the highest among all the systems shown in Table 5. The spent activated carbon can be easily regenerated. There are many techniques which are adopted for this purpose such as pH reversal [29], addition of alcohol [45,46], thermal treatment [47] and acetone and isopropanol [48].

4. Conclusion

Removal of four reactive dyes using a hybrid separation process consisting of adsorption and MF has been presented in this work. Following are the major conclusions:

(i) Maximum adsorption of reactive dyes on activated carbon at lower pH, 2–5.
(ii) One gram per litre adsorbent dose was good enough to remove more than 99% of reactive yellow and brown dyes up to a concentration of 150 mg/L. At 150 mg/L concentration, 85% of reactive red and 80% of reactive black were removed with 1 g/L adsorbent dose. Trial runs showed that more than 99% of these dyes could be removed with adsorbent dose 1.5 g/L.
(iii) Maximum adsorption capacity was 130–152 mg/g for different reactive dyes.
(iv) Presence of electrolyte up to 120 g/L marginally affects the adsorption performance.
(v) Strong hydrogen bonding and hydrophobic interaction between dye and carbon surface were more dominant mechanism compared to electrostatic interactions during adsorption.
(vi) Flux decline during MF was due to formation of cake layer by rejected carbon particles.
(vii) Steady state was attained within 15 min in the experiments under total recycle mode for all the dyes.

(viii) Size of the dyes played important role in membrane fouling. Reactive black having the larger formed a thicker cake layer resulting to the lowest permeate flux.
(ix) Among five washing protocols tested, acid–alkali treatment was found to be the best.
(x) Throughput of the process was remarkably high, 8.1×10^{-4}–1.2×10^{-3} L/m^2 h Pa.

Acknowledgement

Authors gratefully acknowledge the grants provided by Central Glass and Ceramic Research Institute, Kolkata under the grant number GC/CMD/Supra-IIT Collaboration/2011 dated, 7th June, 2011. Authors would also like to thank Mr Sourav Mondal and Mr Bhaskar Charan Bhuniya for their contribution towards this work.

References

[1] H. Wang, J. Qiang Su, X.W. Zheng, Y. Tian, X.J. Xiong, T.L. Zheng, Bacterial decolorization and degradation of the reactive dye Reactive Red 180 by Citrobacter sp. CK3, Int. Biodeterior. Biodegrad. 63 (2009) 395–399.
[2] T.Y. Chen, C.M. Kao, A. Hong, C.E. Lin, S.H. Liang, Application of ozone on the decolorization of reactive dyes—Orange-13 and Blue-19, Desalination 249(3) (2009) 1238–1242.
[3] R. Gogate, A.B. Pandit, A review of imperative technologies for wastewater treatment II: Hybrid methods, Adv. Environ. Res. 8(3–4) (2004) 553–597.
[4] S. Papić, N. Koprivanac, A.L. Božić, D. Vujević, S.K. Dragičević, H. Kušić, I. Peternel, Advanced oxidation processes in azo dye wastewater treatment, Water Environ. Res. 78(6) (2006) 572–579.
[5] C.M. Kao, M.S. Chou, W.L. Fang, B.W. Liu, B.R. Huang, Regulating colored textile wastewater by 3/31 wavelength ADMI methods in Taiwan, Chemosphere 44(5) (2001) 1055–1063.
[6] P. Anielak, S. Wiktorowski, Oxidation of selected, metal-complexed organic dyes with hydrogen peroxide and sodium hypochlorite, Przem. Chem. 82(8–9) (2003) 995–998.
[7] R. Jiraratananon, A. Sungpet, P. Luangsowan, Performance evaluation of nanofiltration membranes for treatment of effluents containing reactive dye and salt, Desalination 130(2) (2000) 177–183.
[8] E. Alventosa-deLara, S. Barredo-Damas, M.I. Alcaina-Miranda, M.I. Iborra-Clar, Ultrafiltration technology with a ceramic membrane for reactive dye removal: Optimization of membrane performance, J. Hazard. Mater. 209–210 (2012) 492–500.
[9] Y.M. Slokar, A.M. Majcen Le Marechal, Methods of decoloration of textile wastewaters, Dyes Pigm. 37(4) (1998) 335–356.
[10] A.B. dos Santos, F.J. Cervantes, J.B. van Lier, Review paper on current technologies for decolourisation of textile wastewaters: Perspectives for anaerobic biotechnology, Bioresour. Technol. 98(12) (2007) 2369–2385.
[11] S.H. Lin, C.F. Peng, Treatment of textile wastewater by electrochemical method, Water Res. 28 (1994) 277–282.
[12] S.H. Lin, C.F. Peng, Continuous treatment of textile wastewater by combined coagulation, electrochemical oxidation and activated sludge, Water Res. 30 (1996) 587–592.
[13] B. Merzouk, B. Gourich, A. Sekki, K. Madani, C. Vial, M. Barkaoui, Studies on the decolorization of textile dye wastewater by continuous electrocoagulation process, Chem. Eng. J. 149 (2009) 207–214.
[14] S.H. Lin, M.L. Chen, Treatment of textile wastewater by chemical methods for reuse, Water Res. 31 (1997) 868–876.
[15] H. Shu, C. Huang, Degradation of commercial azo dyes in water using ozonation and UV enhanced ozonation process, Chemosphere 31 (1995) 3813–3825.
[16] H. Abdul Aziz, S. Alias, M.N. Adlan, A.H. Faridah, M. Asaari, S. Zahari, Colour removal from landfill leachate by coagulation and flocculation processes, Bioresour. Technol. 98 (2007) 218–220.
[17] I. Koyuncu, Reactive dye removal in dye/salt mixtures by nanofiltration membranes containing vinylsulphone dyes: Effects of feed concentration and cross flow velocity, Desalination 143 (2002) 243–253.
[18] T. Kim, C. Park, S. Kim, Water recycling from desalination and purification process of reactive dye manufacturing industry by combined membrane filtration, J. Cleaner Prod. 13(8) (2005) 779–786.
[19] D.B. Voncina, A. Majcen-Le-Marechal, Reactive dye decolorization using combined ultrasound/H_2O_2, Dyes Pigm. 59(2) (2003) 173–179.
[20] I. Poulios, I. Tsachpinis, Photodegradation of the textile dye Reactive Black 5 in the presence of semiconducting oxides, J. Chem. Technol. Biotechnol. 74 (1999) 349–357.
[21] M. Li, J. Li, H. Sun, Decolorizing of azo dye Reactive red 24 aqueous solution using exfoliated graphite and H_2O_2 under ultrasound irradiation, Ultrason. Sonochem. 15 (2008) 717–723.
[22] http://www.worlddyevariety.com/reactive-dyes/reactive-brown-10.html
[23] K. Vanommeslaeghe, E.P. Raman, A.D. MacKerell Jr., Automation of the CHARMM General Force Field (CGENFF) II: Assignment of bonded parameters and partial atomic charges, J. Chem. Inf. Model. 52 (2012) 3155–3168.
[24] V. Zoete, M.A. Cuendet, A. Grosdidier, O. Michielin, SwissParam: A fast force field generation tool for small organic molecules, J. Comput. Chem. 32(11) (2011) 2359–2368.
[25] A.D. MacKerell Jr., D. Bashford, M. Bellott, R.L. Dunbrack Jr., J.D. Evanseck, M.J. Field, S. Fischer, J. Gao, H. Guo, S. Ha, D. Joseph-McCarthy, L. Kuchnir, K. Kuczera, F.T.K. Lau, C. Mattos, S. Michnick, T. Ngo, D.T. Nguyen, B. Prodhom, W.E. Reiher III, B. Roux, M. Schlenkrich, J.C. Smith, R. Stote, J. Straub, M. Watanabe, J. Wiórkiewicz-Kuczera, D. Yin, M. Karplus, All-atom emperical potential for molecular modeling and dynamics studies of proteins, J. Phys. Chem. B 102 (1998) 3586–3616.
[26] B.R. Brooks, C.L. Brooks III, A.D. Mackerell Jr., L. Nilsson, R.J. Petrella, B. Roux, Y. Won, G. Archontis,

C. Bartels, S. Boresch, A. Caflisch, L. Caves, Q. Cui, A.R. Dinner, M. Feig, S. Fischer, J. Gao, M. Hodoscek, W. Im, K. Kuczera, T. Lazaridis, J. Ma, V. Ovchinnikov, E. Paci, R.W. Pastor, C.B. Post, J.Z. Pu, M. Schaefer, B. Tidor, R.M. Venable, H.L. Woodcock, X. Wu, W. Yang, D.M. York, M. Karplus, CHARMM: The biomolecular simulation program, J. Comp. Chem. 30 (2009) 1545–1614.

[27] A. Rafique, M.A. Awan, A. Wasti, I.A. Qazi, M. Arshad, Removal of fluoride from drinking water using modified immobilized activated alumina, J. Chem. (2013), 7 pp. (Article ID 386476), doi: 10.1155/2013/386476.

[28] X. Yang, B. Al-Duri, Kinetic modeling of liquid-phase adsorption of reactive dyes on activated carbon, J. Colloid Interface Sci. 287 (2005) 25–34.

[29] C. Namasivayam, D. Kavitha, Removal of Congo Red from water by adsorption onto activated carbon prepared from coir pith, an agricultural solid waste, Dyes Pigm. 54 (2002) 47–58.

[30] S. Senthilkumaar, P. Kalaamani, K. Porkodi, P.R. Varadarajan, C.V. Subburaam, Adsorption of dissolved Reactive red dye from aqueous phase onto activated carbon prepared from agricultural waste, Bioresour. Technol. 97 (2006) 1618–1625.

[31] Y.S. Al-Degs, M.I. El-Barghouthi, A.H. El-Sheikh, G.M. Walker, Effect of solution pH, ionic strength, and temperature on adsorption behavior of reactive dyes on activated carbon, Dyes Pigm. 77 (2008) 16–23.

[32] G. Newcombe, M. Drikas, Adsorption of NOM activated carbon: Electro-static and non-electrostatic effects, Carbon 35 (1997) 1239–1250.

[33] G. Newcombe, C. Donati, M. Drikas, R. Hayes, Adsorption onto activated carbon: Electrostatic and non-electrostatic interactions, Water Suppl. 14 (1996) 129–144.

[34] R.J. Martin, W.J. Ng, The repeated exhaustion and chemical regeneration of activated carbon, Water. Res. 21(8) (1987) 961–965.

[35] S.S. Popovic, S.D. Milanovic, M.D. Ilicic, N.L. Lukic, I.M. Sijacki, Flux recovery of ceramic tubular membranes fouled with whey proteins: Some aspects of membrane cleaning, APTEFF 39 (2008) 101–109.

[36] N. Porcelli, S. Judd, Chemical cleaning of potable water membranes: A review, Sep. Purif. Technol. 71(2) (2010) 137–143.

[37] J. Lee, S. Choi, R. Thiruvenkatachari, W. Shim, H. Moon, Submerged microfiltration membrane coupled with alum coagulation/powdered activated carbon adsorption for complete decolorization of reactive dyes, Water. Res. 40 (2006) 435–444.

[38] F. Harrelkas, A. Azizi, A. Yaacoubi, A. Benhammou, M.N. Pons, Treatment of textile dye effluents using coagulation–flocculation coupled with membrane processes or adsorption on powdered activated carbon, Desalination 235 (2009) 330–339.

[39] J. Huang, C. Zhou, G. Zeng, X. Li, J. Niu, H. Huang, L. Shi, S. He, Micellar-enhanced ultrafiltration of methylene blue from dye wastewater via a polysulfone hollow fiber membrane, J. Membr. Sci. 365 (2010) 138–144.

[40] A.L. Ahmad, S.W. Puasa, M.M.D. Zulkali, Micellar-enhanced ultrafiltration for removal of reactive dyes from an aqueous solution, Desalination 191 (2006) 153–161.

[41] A.L. Ahmad, S.W. Puasa, Reactive dyes decolourization from an aqueous solution by combined coagulation/micellar-enhanced ultrafiltration process, Chem. Eng. J. 132 (2007) 257–265.

[42] S.U. Hong, M.D. Miller, M.L. Bruening, Removal of dyes, sugars, and amino acids from NaCl solutions using multilayer polyelectrolyte nanofiltration membranes, Ind. Eng. Chem. Res. 45 (2006) 6284–6288.

[43] C. Fersi, M. Dhahbi, Treatment of textile plant effluent by ultrafiltration and/or nanofiltration for water reuse, Desalination 222 (2008) 263–271.

[44] A. Akbari, J.C. Remigy, P. Aptel, Treatment of textile dye effluent using a polyamide-based nanofiltration membrane, Chem. Eng. Process. 41 (2002) 601–609.

[45] J. Chern, C. Wu, Desorption of dye from activated carbon beds: Effects of temperature, pH, and alcohol, Water. Res. 35(17) (2001) 4159–4165.

[46] W. Tanthapanichakoon, P. Ariyadejwanich, P. Japthong, K. Nakagawa, S.R. Mukai, H. Tamon, Adsorption–desorption characteristics of phenol and reactive dyes from aqueous solution on mesoporous activated carbon prepared from waste tires, Water. Res. 39 (2005) 1347–1353.

[47] W. Li, Q. Yue, B. Gao, Z. Ma, Y. Li, H. Zhao, Preparation and utilization of sludge-based activated carbon for the adsorption of dyes from aqueous solutions, Chem. Eng. J. 171 (2011) 320–327.

[48] P. Lu, H. Lin, W. Yu, J. Chern, Chemical regeneration of activated carbon used for dye adsorption, J. Taiwan Inst. Chem. Eng. 42 (2011) 305–311.